

Ferromagnetic semiconductors based upon AlGaP

M. E. Overberg,^{a)} G. T. Thaler, R. M. Frazier, C. R. Abernathy, and S. J. Pearton
Department of Materials Science and Engineering, University of Florida, Gainesville, Florida 32611

R. Rairigh, J. Kelly, N. A. Theodoropoulou, and A. F. Hebard
Department of Physics, University of Florida, Gainesville, Florida 32611

R. G. Wilson
Consultant, Stevenson Ranch, California 91381

J. M. Zavada
US Army Research Office, Research Triangle Park, North Carolina 27709

(Presented on 14 November 2002)

Ion implantation of Mn or Cr at concentrations of 1–5 at. % were performed in $\text{Al}_x\text{Ga}_{1-x}\text{P}$ ($x = 0.24, 0.38$) epilayers grown by gas source molecular beam epitaxy. Ferromagnetic-like ordering above 100 K for Cr and 300 K for Mn was observed in superconducting quantum interference device measurements. Structural characterization revealed no second phases that could influence the measured magnetic properties. As the AIP mole fraction in the $\text{Al}_x\text{Ga}_{1-x}\text{P}$ layers increased, the magnetic ordering temperatures were generally observed to increase, while the calculated magnetic moment decreased. Mn appears to be a more promising choice than Cr for high temperature ferromagnetism in AlGaP. © 2003 American Institute of Physics. [DOI: 10.1063/1.1556247]

INTRODUCTION

While mean-field theories predict relatively low Curie temperatures (<110 K) for $(\text{Ga,Mn})\text{P}$,^{1–3} recent experiments show ferromagnetism above 300 K.^{3–5} In other respects, the magnetic behavior of the $(\text{Ga,Mn})\text{P}$ was consistent with mean-field predictions. For example, the magnetization versus temperature plots showed a more classical concave shape⁶ than observed with many diluted magnetic semiconductor (DMS) materials. In addition, the Curie temperature was strongly influenced by the carrier density and type in the material, with highly p -type samples showing much higher values than n -type or undoped samples. Finally, the Curie temperature increased with Mn concentration up to ~6 at. % and decreased at higher concentrations. No secondary phases or clusters could be detected by transmission electron microscopy, x-ray diffraction, or selected area diffraction patterns. Similar results were achieved in samples in which the Mn was incorporated during molecular beam epitaxy (MBE) growth or directly implanted with Mn.

GaP is a particularly attractive host material for spintronic applications because it is almost lattice matched to Si. One can therefore envision integration of $(\text{Ga,Mn})\text{P}$ spintronic magnetic sensors or data storage elements to form fast nonvolatile magnetic random access memories (MRAM) and the possibility of integrating ferromagnetic semiconductors with existing Si microelectronics. Although it has an indirect band gap, it can be made to luminescence through addition of isoelectric dopants such as nitrogen or else one could employ the direct band-gap ternary InGaP, which is lattice matched to GaAs. An immediate application of the DMS counterparts to the component binary and ternary materials

in this system would be to add spin functionality to all of these devices. A further advantage to the wide band-gap phosphides is that they exhibit room temperature ferromagnetism even for relatively high growth temperatures during MBE. The InGaAlP system, with its wide band-gap binary (GaP, AlP) and ternary (InGaP, AlGaP, AlInP) components, is used for devices such as visible light-emitting diodes and laser diodes (the band gap ranges from 1.9 eV for $\text{In}_{0.49}\text{Ga}_{0.51}\text{P}$ which is lattice matched to GaAs substrates to 2.3 eV for $(\text{Al}_x\text{Ga}_{1-x})_{0.51}\text{In}_{0.49}\text{P}$ with $x = 0.66$), heterojunction bipolar transistors, and high electron mobility transistors. The binary compounds AlP and AlAs are unstable in air and oxidize rapidly unless covered with a capping layer.

Ferromagnetism above room temperature in $(\text{Ga,Mn})\text{P}$ has been reported for two different methods of Mn incorporation, namely ion implantation and doping during MBE growth. The implantation process is an efficient one for rapidly screening whether particular combinations of magnetic dopants and host semiconductors are promising in terms of ferromagnetic properties. We have used implantation to introduce ions such as Mn, Fe, and Ni into a variety of substrates, including GaN, SiC, and GaP.^{7–11} In this article we report on the magnetic and structural properties of Mn and Cr-implanted AlGaP, as a function of the transition metal concentration.

EXPERIMENT

$\text{Al}_x\text{Ga}_{1-x}\text{P}:\text{C}$ layers ($x = 0.24–0.38$) were grown on undoped GaP substrates using gas source molecular beam epitaxy. The Al was provided by a dimethylethylamine alane source using ultrapure He as a carrier gas. The Ga was provided by a shuttered effusion oven charged with 7 N (99.999 99% pure) material. The C for electrical doping was provided by CBr_4 pyrolyzed at the substrate surface. Ther-

^{a)}Electronic mail: mover@mse.ufl.edu

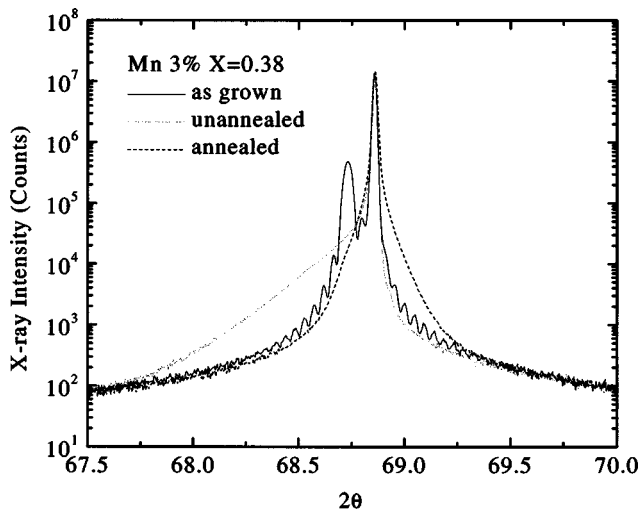


FIG. 1. A representative XRD ω - 2θ rocking curve measurement of $\text{Al}_{0.38}\text{Ga}_{0.62}\text{P:C}$ [optimized to the GaP (400) plane] before and after Mn implantation ($3 \times 10^{16} \text{ cm}^{-2}$) and after subsequent annealing at 700 °C.

mally cracked PH_3 provided the group V species. A growth temperature of 650 °C was used for the films, whose thickness was typically 0.5 μm . The p -type doping concentration was $\sim 5 \times 10^{18} \text{ cm}^{-3}$ for the epilayers, as measured by the Hall effect. Implants of 250 keV Cr^+ or Mn^+ ions were performed at 350 °C at doses from $(1 \text{ to } 5) \times 10^{16} \text{ cm}^{-2}$. These doses correspond to peak volume concentrations of 1–5 at. % at a distance of $\sim 1500 \text{ \AA}$ from the surface. Following implantation, the samples were annealed at 700 °C for 5 min under flowing N_2 to remove lattice disorder. Structural analysis via high-resolution x-ray diffraction was performed in a Philips MPD X'pert diffractometer. Magnetic measurements were performed in a Quantum Design superconducting quantum interference device (SQUID) magnetic properties measurement system.

RESULTS AND DISCUSSION

Figure 1 shows a representative ω - 2θ rocking curve of $\text{Al}_{0.38}\text{Ga}_{0.62}\text{P:C}$ about the (400) peak of GaP before and after Mn implantation at a dose of $3 \times 10^{16} \text{ cm}^{-2}$ and following subsequent annealing. All peaks correspond to those expected from the epilayer and substrate, with no peaks due to second phases such as $\text{Mn}_x\text{Ga}_{1-x}$ (which is ferromagnetic with a Curie temperature $> 300 \text{ K}$ for $0.55 < x < 0.6$)^{12,13} or Mn_xP_y (e.g., Mn_3P and Mn_2P are antiferromagnetic, while MnP is ferromagnetic with a Curie temperature of 291 K¹⁴) being observed. The as-grown sample exhibits excellent crystal quality and an excellent interface as is evident from the Pendellosung fringes, while the implant sample shows a much-broadened peak due to the introduction of lattice disorder. Annealing produces a significant repair of this disorder and a shift in the peak, which may be due to the DMS phases. Similar results were observed for Cr-implanted samples.

Figure 2 shows some representative M - H plots as a function of measurement temperature for a representative $\text{Al}_{0.38}\text{Ga}_{0.62}\text{P:C}$ sample implanted with $5 \times 10^{16} \text{ cm}^{-2}$ Mn and subsequently annealed at 700 °C. There is still an appreciable

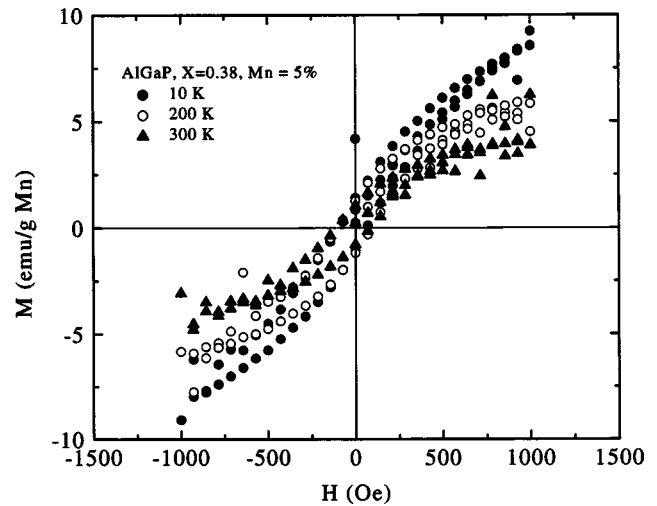


FIG. 2. SQUID magnetometer measurements of magnetization (in emu/g Mn) as a function of applied field for Mn-implanted ($5 \times 10^{16} \text{ cm}^{-2}$) $\text{Al}_{0.38}\text{Ga}_{0.62}\text{P:C}$ annealed at 700 °C, as a function of measurement temperature.

able magnetization signal present at 300 K. Diamagnetic contributions from the substrate have been subtracted out. At low temperatures, the saturation moment, $M_0 = g \mu_B S$, was calculated to range from 0.13 to 0.23 Bohr magnetons (μ_B) per Mn ion depending on the Mn dose and the Al concentration. This value is approximately a factor of 25 less than the value expected from the half-filled d band of divalent Mn, which could be due to several factors. These include strong antiferromagnetic coupling among the more closely spaced randomly positioned Mn ions, disorder effects that give rise to a wide distribution of exchange couplings, and hopping integrals. Therefore the participation of many of the Mn ions in the ferromagnetism would be excluded, causing the substitutional fraction of Mn ions to be unknown.¹⁵

Similar trends were observed for Cr-implanted samples, with saturation moments reaching a maximum value of 0.14 Bohr magnetons per Cr ion. Theoretical work by Sato and Katayama-Yoshida have predicted that Cr will produce the highest Curie temperatures in GaP ($> 500 \text{ K}$ for Cr concentrations above 12 at. %).¹⁶ These calculations are based upon a local spin-density approximation which assumes the magnetic ions are randomly substituted for Ga atoms, and no additional effects due to carrier doping are taken into account.¹⁶

Figure 3 shows M - T data for $\text{Al}_{0.38}\text{Ga}_{0.62}\text{P:C}$ implanted with $5 \times 10^{16} \text{ cm}^{-2}$ Mn and $3 \times 10^{16} \text{ cm}^{-2}$ Cr. A general trend we observed (with various concentrations of Mn and Cr) was that as the Al concentration in the sample increased, the Curie temperature (defined as the temperature at which M went to zero) increased but the calculated moment decreased. This is most likely related to the higher bond strength of the Al-rich compositions, leading to a lower concentration of Ga vacancies for the implanted Mn to occupy and contribute to the ferromagnetism.¹⁷ The overall shape of the M - T plots is non-Brillouin-like, as suggested theoretically in disordered systems.^{6,15,18} Although no second phases were observed within the detection limits of the x-ray diffraction (XRD), we

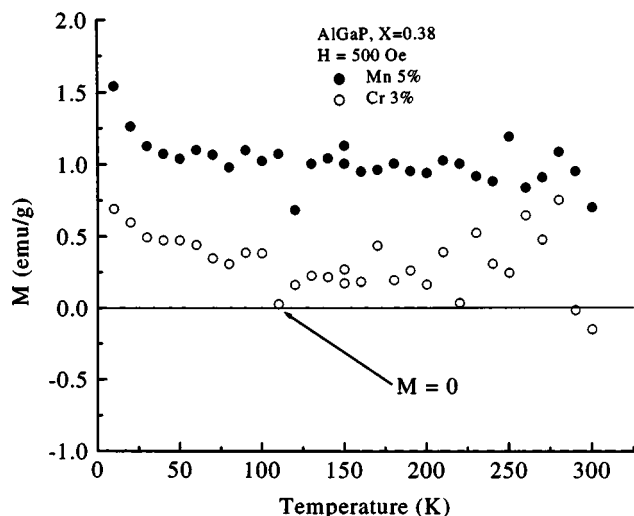


FIG. 3. SQUID magnetometer measurements of magnetization (in emu/g) as a function of temperature for a dose of $5 \times 10^{16} \text{ cm}^{-2}$ Mn and $3 \times 10^{16} \text{ cm}^{-2}$ Cr implanted into $\text{Al}_{0.38}\text{Ga}_{0.62}\text{P:C}$ ($H=500 \text{ Oe}$).

cannot completely rule out the existence of clustering. Such small clusters would most likely be superparamagnetic, i.e., thermal energy would randomize the magnetization of individual clusters. Zero field cooled/field cooled measurements did not indicate the presence of any blocking temperature that could be associated with superparamagnetic behavior arising from undetected magnetic second phase clusters.¹⁹

SUMMARY AND CONCLUSIONS

The structural and magnetic properties of p -type $\text{Al}_x\text{Ga}_{1-x}\text{P:C}$ implanted with Mn or Cr were investigated. No second phases were observed to form under our implantation and annealing conditions. The magnetic characterization showed ferromagnetic-like ordering at $\leq 100 \text{ K}$ for Cr and $> 300 \text{ K}$ for Mn, in contrast to some theoretical predictions which suggested Cr may have very high Curie temperatures in the AlGaP system. The use of AlGaP rather than GaP as the host semiconductor did not lead to a major increase in ferromagnetic ordering temperature for either transition metal dopant.

ACKNOWLEDGMENTS

The work at UF was partially supported by the U.S. Army Research Office under Grant No. ARO-DAAG55-98-1-0216 and by the National Science Foundation under Grant Nos. DMR-9705224 and DMR-0101438.

- ¹T. Dietl, H. Ohno, F. Matsukura, J. Cibert, and D. Ferrand, *Science* **287**, 1019 (2000).
- ²T. Dietl, H. Ohno, and F. Matsukura, *Phys. Rev. B* **63**, 195205 (2001).
- ³T. Dietl, *J. Appl. Phys.* **89**, 7437 (2001).
- ⁴N. Theodoropoulou, A. F. Hebard, M. E. Overberg, C. R. Abernathy, S. J. Pearton, S. N. G. Chu, and R. G. Wilson, *Phys. Rev. Lett.* **89**, 107203 (2002).
- ⁵M. E. Overberg, B. P. Gila, G. T. Thaler, C. R. Abernathy, S. J. Pearton, N. Theodoropoulou, K. T. McCarthy, S. B. Arnason, A. F. Hebard, S. N. G. Chu, R. G. Wilson, J. M. Zavada, and Y. D. Park, *J. Vac. Sci. Technol. B* **20**, 969 (2002).
- ⁶R. N. Bhatt, M. Berciu, M. D. Kennett, and X. Wan, *J. Supercond.* **15**, 71 (2002).
- ⁷N. Theodoropoulou, K. P. Lee, M. E. Overberg, S. N. G. Chu, A. F. Hebard, C. R. Abernathy, S. J. Pearton, and R. G. Wilson, *J. Nanosci. Nanotech.* **1**, 1012 (2001).
- ⁸N. Theodoropoulou, A. F. Hebard, M. E. Overberg, C. R. Abernathy, S. J. Pearton, S. N. G. Chu, and R. G. Wilson, *Appl. Phys. Lett.* **78**, 3475 (2001).
- ⁹N. Theodoropoulou, A. F. Hebard, M. E. Overberg, S. J. Pearton, C. R. Abernathy, S. N. G. Chu, and R. G. Wilson, *J. Appl. Phys.* **91**, 7499 (2002).
- ¹⁰N. Theodoropoulou, M. E. Overberg, S. N. G. Chu, A. F. Hebard, C. R. Abernathy, R. G. Wilson, J. M. Zavada, K. P. Lee, and S. J. Pearton, *Phys. Status Solidi B* **228**, 337 (2001).
- ¹¹N. Theodoropoulou, A. F. Hebard, S. N. G. Chu, M. E. Overberg, C. R. Abernathy, S. J. Pearton, R. G. Wilson, and J. M. Zavada, *Appl. Phys. Lett.* **79**, 3452 (2001).
- ¹²M. Tanaka, J. P. Harbison, J. DeBoeck, T. Sands, B. Phillips, T. L. Cheeks, and V. G. Keramidas, *Appl. Phys. Lett.* **62**, 1565 (1993).
- ¹³M. Tanaka, J. P. Harbison, T. Sands, B. Phillips, T. L. Cheeks, J. DeBoeck, L. T. Florez, and V. G. Keramidas, *Appl. Phys. Lett.* **63**, 696 (1993).
- ¹⁴Y. Shapira, N. F. Oliveira, C. C. Becerrand, and S. Foner, *Phys. Rev.* **17**, 929 (1960).
- ¹⁵M. Berciu and R. N. Bhatt, *Phys. Rev. Lett.* **87**, 107203 (2001).
- ¹⁶K. Sato and H. Katayama-Yoshida, *Jpn. J. Appl. Phys., Part 2* **40**, L485 (2001).
- ¹⁷J. S. Williams, *Mater. Sci. Eng., A* **213**, 9 (1998).
- ¹⁸A. Kaminski and S. Das Sarma, *Phys. Rev. Lett.* **88**, 247202 (2002).
- ¹⁹P. Xiong, G. Xiao, J. Q. Wang, J. S. Jiang, and C. L. Chien, *Phys. Rev. Lett.* **69**, 3220 (1992).